

Metal-ligand ring aromaticity in a 2D coordination polymer used as a photosensitive electronic device

Faruk Ahmed,^a Sourav Ranjan Ghosh,^{b,d} Soumi Halder,^c Surajit Guin,^b Seikh Mafiz Alam,^a Partha Pratim Ray,*^c Atish Dipankar Jana*^b and Mohammad Hedayetullah Mir*^a

^a*Department of Chemistry, Aliah University, New Town, Kolkata 700 156. Email: chmmir@gmail.com*

^b*Department of Physics, Behala College, Parnasree, Kolkata, 700 060, India. Email: atishdipankarjana@yahoo.in*

^c*Department of Physics, Jadavpur University, Jadavpur, Kolkata 700 032, India.*

^d*Department of Physics, Heritage Institute of Technology Kolkata 700 107, India*

Supporting Information

1. List of Figures

Fig. S1: A part of 2D structural network of **1** showing fes Shubnikov plane net (4.8^2)

Fig. S2: H-bonding pattern in 2D sheet of compound **1**

Fig. S3: DFT computed interaction energy of inter-layer $\pi\cdots\pi$ interaction, and two C-H $\cdots\pi$ interactions (for one H \cdots centroid distance is 2.79Å and for other it is 3.0Å) of **1**

Fig S4: C-H $\cdots\pi$ (metal-ligand ring) and $\pi\cdots\pi$ interactions in **1**.

Fig S5: Variation of NICS value with height from mean plane at the center and at point 1 of the 14-member ring. Basis set dependency of the results have been shown in the inset.

Fig. S6: TGA plot of compound **1** under N_2 atmosphere

Fig. S7: Powder X-ray diffraction patterns of simulated **1** (black) and as-synthesized **1** (red).

Fig. S8: FESEM image of compound **1**.

Fig. S9: (a) 2D fingerprint plot (full); (b) 2D fingerprint plot with C \cdots H/H \cdots C interactions (c) 2D fingerprint plot with O \cdots H/H \cdots O interactions (d) 2D fingerprint plot with C \cdots C interactions highlighted in colour.

Fig. S10: ELF- σ and ELF- π over the 14 member ring

2. List of Tables

Table S1: Crystal data and refinement parameters for compound **1**

Table S2: Selected bond lengths and bond angles in **1**

Table S3: Hydrogen bonding interactions in **1**

Table S4: C-H $\cdots\pi$ interactions in **1**

Table S5: $\pi\cdots\pi$ interactions in **1**

Table S6: Variation of NICS values (in ppm) with height at different points of the 14 member metal-ligand ring

Table S7: Calculated NICS(0) values at the 14 member metal-ligand ring center and at point(1) for different level of theory

Table S8: Component wise variation of NICS values with height at point (1)

Table S9: Basis set superposition error (BSSE) corrected binding energies of the C-H $\cdots\pi$ interaction involving 14-member metal-ligand ring and 4-phpy computed at HF/6-31G(d,p) and HF/6-311++G(d,p) level of theory

Table S10: Binding energies of the C-H $\cdots\pi$ interaction involving 14-member metal-ligand ring and 4-phpy, $\pi\cdots\pi$ and two different C-H $\cdots\pi$ interaction among 4-phpy molecules computed at DFT/M06-2X/6-31G(d,p) level of theory

3. References

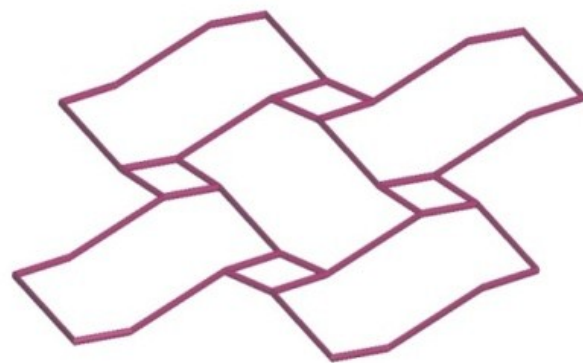


Fig. S1. A part of 2D structural network of **1** showing fes Shubnikov plane net (4.8^2).

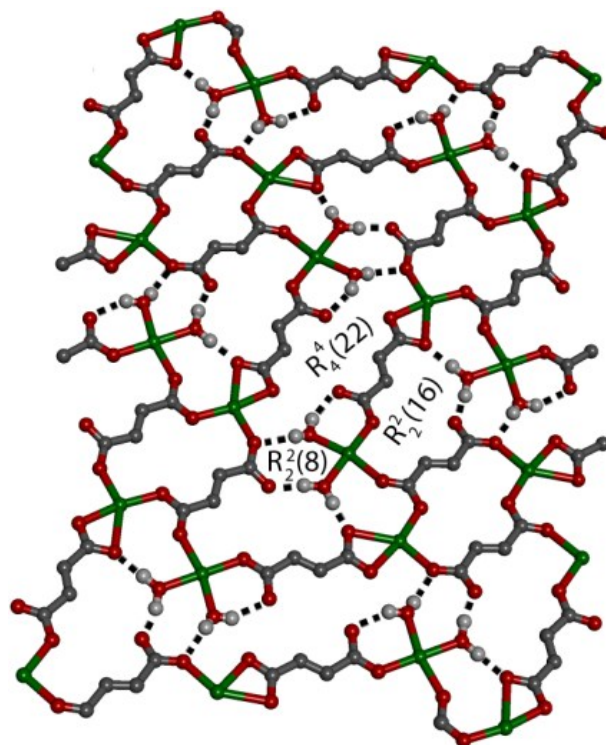


Fig. S2. H-bonding pattern in 2D sheet of compound **1**.

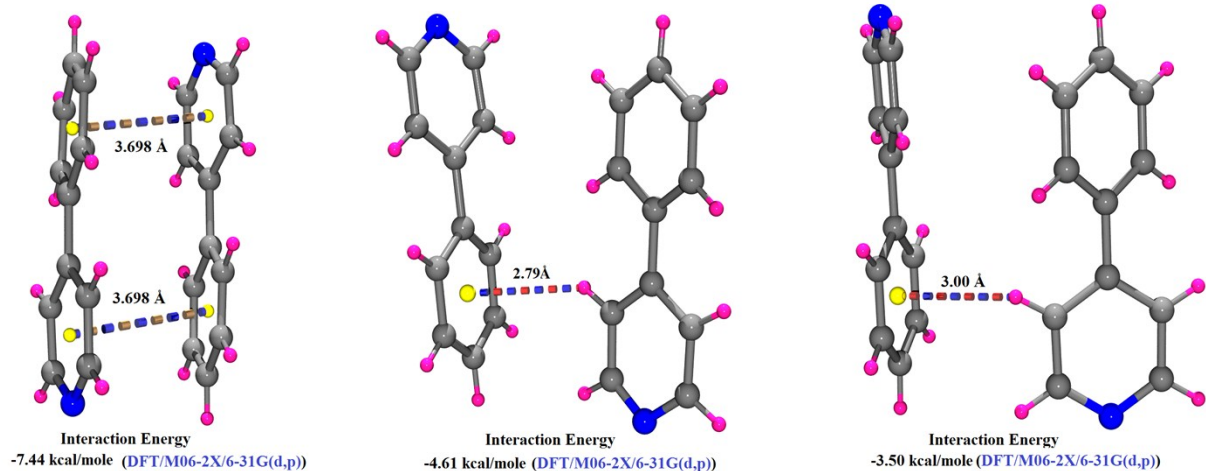


Fig. S3. DFT computed interaction energy of inter-layer $\pi\cdots\pi$ interaction, and two C-H $\cdots\pi$ interactions (for one H \cdots centroid distance is 2.79 Å and for other it is 3.0 Å) of **1**.

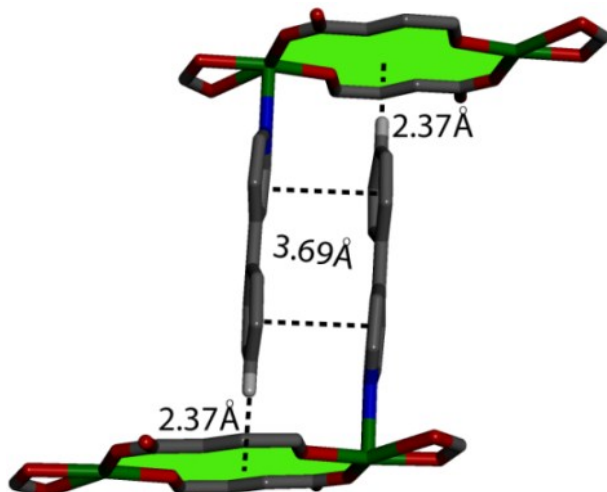


Fig. S4. C-H $\cdots\pi$ (metal-ligand ring) and $\pi\cdots\pi$ interactions in **1**.

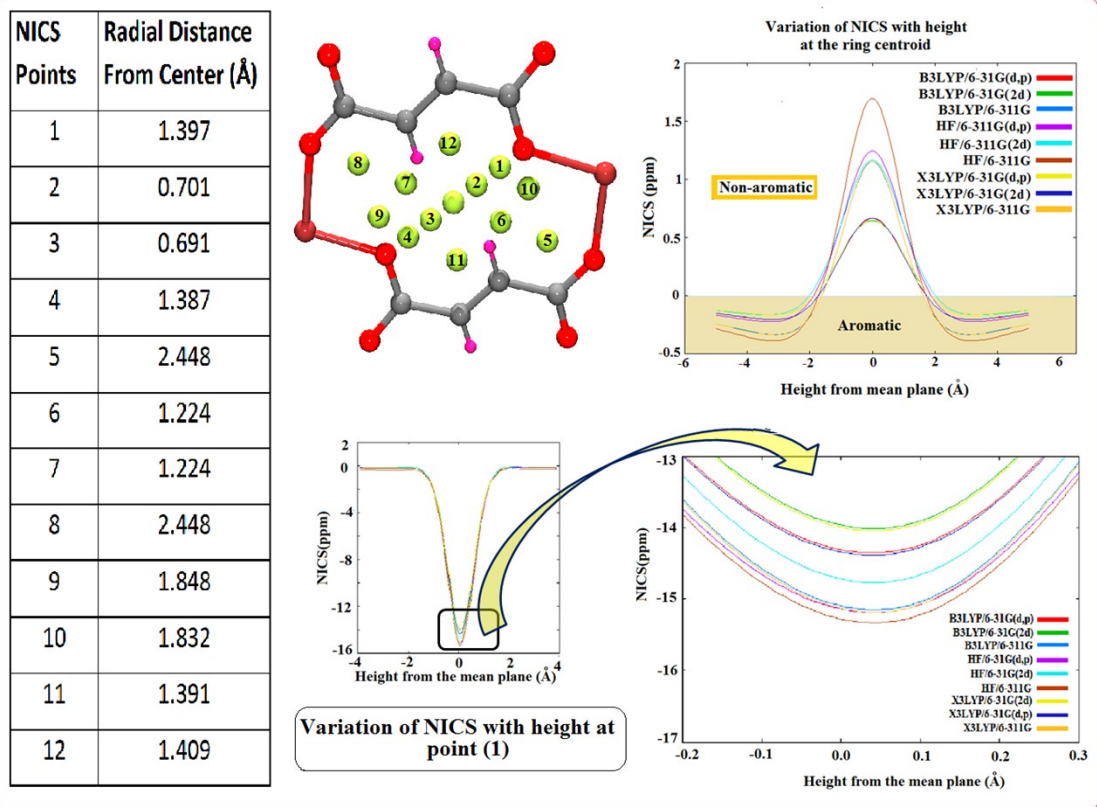


Fig. S5. Variation of NICS value with height from mean plane at the center and at point 1 of the 14-member ring. Basis set dependency of the results have been shown in the inset.

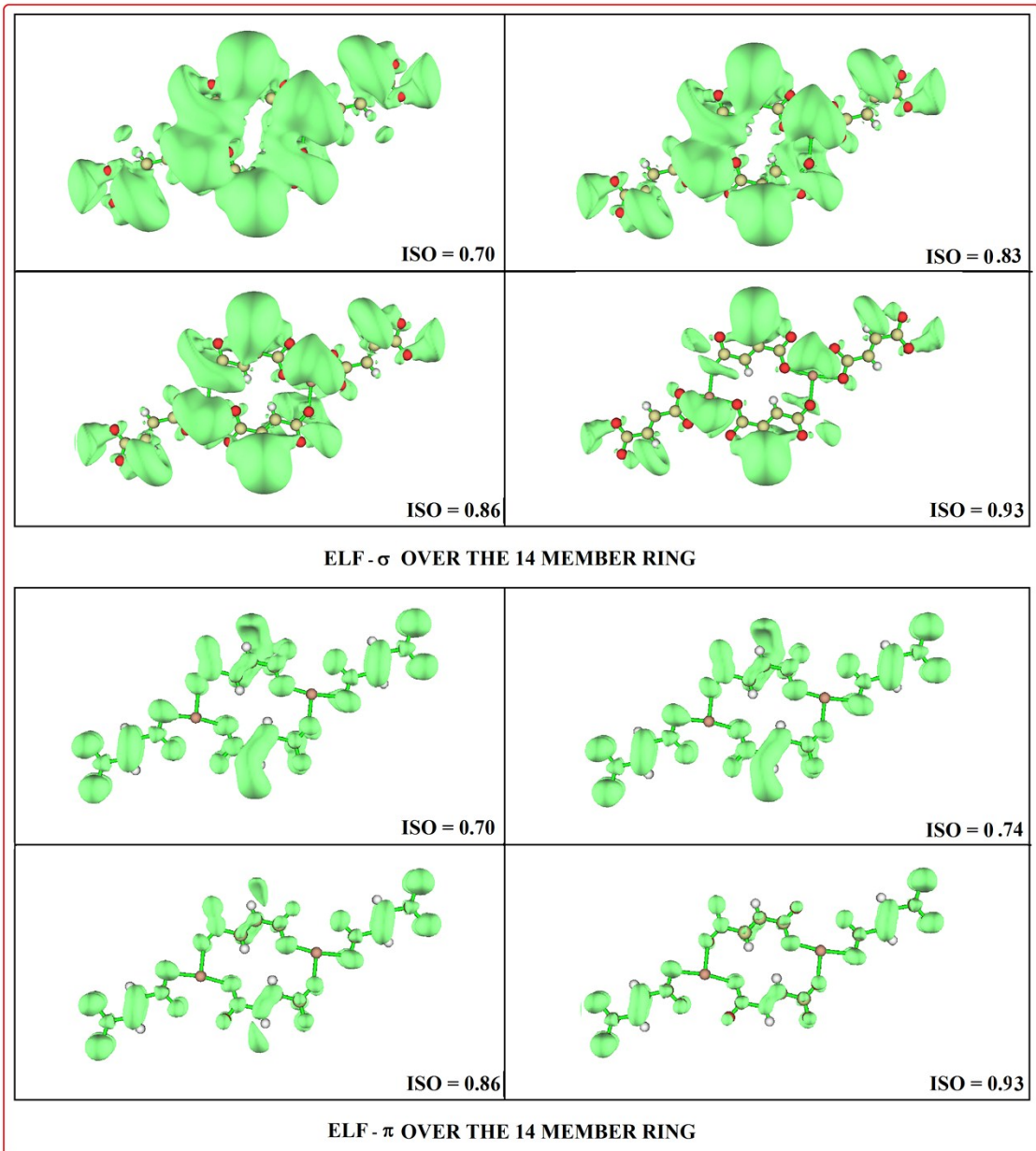


Fig. S6. ELF- σ and ELF- π over the 14 member ring

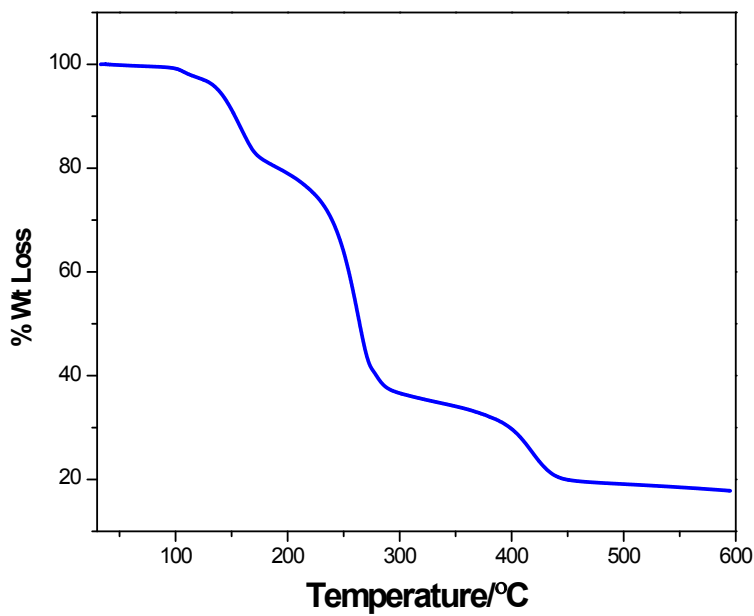


Fig. S7. TGA plot of compound **1** under N_2 atmosphere.

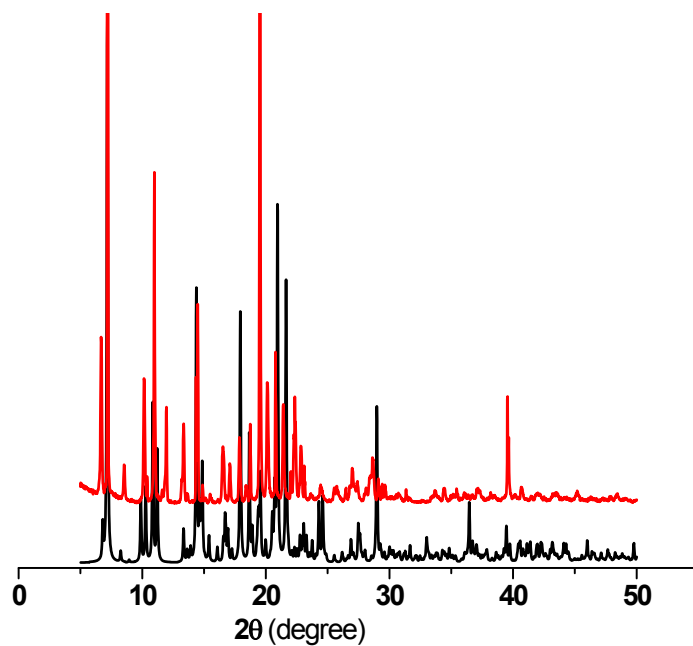


Fig. S8. Powder X-ray diffraction patterns of simulated **1** (black) and as-synthesized **1** (red).

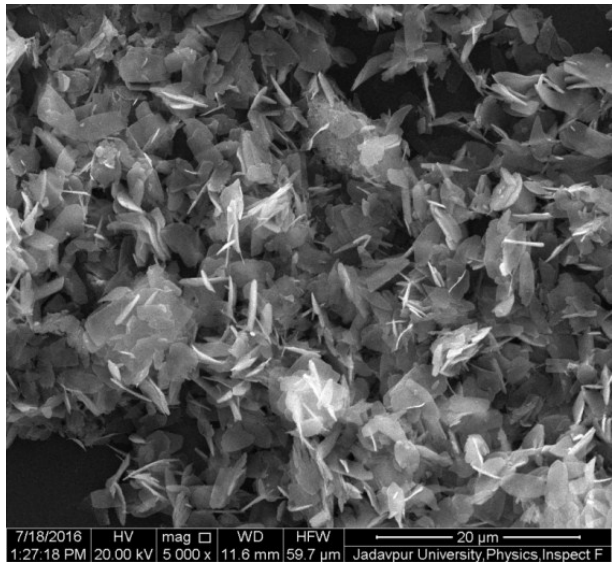


Fig. S9. FESEM image of compound 1.

The Hirshfeld Surface Analysis:

Hirshfeld surfaces¹⁻³ and the associated two-dimensional (2D) fingerprint⁴⁻⁶ plots were calculated with the help of Crystal Explorer⁷ using cif of the complex. The normalized contact distance (d_{norm}) based on d_e and d_i is given by

$$d_{norm} = \frac{(d_i - r_i^{vdW})}{r_i^{vdW}} + \frac{(d_e - r_e^{vdW})}{r_e^{vdW}}$$

where r_i^{vdW} and r_e^{vdW} are the van der Waals radii of the atoms; d_e is the distance from the point to the nearest nucleus external to the surface and d_i is the distance to the nearest nucleus internal to the surface. Bright red spots highlight shorter contacts, white areas represent contacts around van der Waals separation, and blue regions are devoid of close contacts in the Hirshfeld surface.

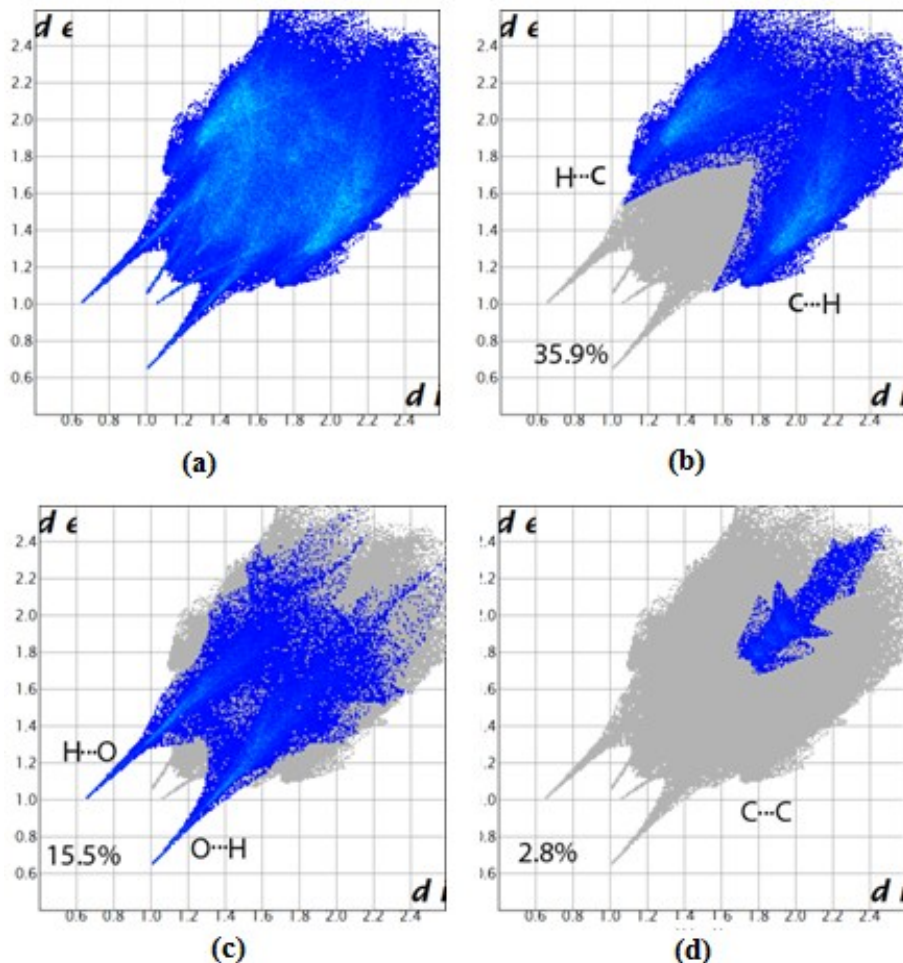


Fig. S10. (a) 2D fingerprint plot (full); (b) 2D fingerprint plot with C···H/H···C interactions (c) 2D fingerprint plot with O···H/H···O interactions (d) 2D fingerprint plot with C···C interactions highlighted in colour.

Table S1 Crystal data and refinement parameters for compound **1**

Formula	C ₅₂ H ₄₄ Zn ₂ N ₄ O ₁₀
Fw	1015.65
cryst syst	Monoclinic
space group	P 2 ₁ /n
a (Å)	13.4470(5)
b (Å)	19.7664(7)
c (Å)	18.1854(6)
α (deg)	90
β (deg)	108.9020(10)
γ (deg)	90
V (Å ³)	4573.0(3)
Z	4
D _{calcd} (g/cm ³)	1.475
μ (mm ⁻¹)	1.115
λ (Å)	0.71073
data [I > 2σ(I)]/params	11360/ 619
GOF on F ²	0.961
final R indices [I > 2σ(I)] ^{a,b}	R1 = 0.0572
	wR2 = 0.1853

[^a]R1 = Σ||F_o| - |F_c||/ Σ|F_o|, wR2 = [Σw(F_o² - F_c²)²/Σw(F_o²)²]^{1/2}.

Table S2 Selected bond lengths and bond angles in **1**

Zn(2)-O(6)	2.049(2)	Zn(1)-O(3)	2.0276(19)
Zn(2)-O(7)	2.078(2)	Zn(1)-O(9)	2.064(2)
Zn(2)-O(8)	2.079(2)	Zn(1)-O(1)	2.101(2)
Zn(2)-O(4)	2.125(2)	Zn(1)-O(2)	2.412(3)
Zn(2)-N(4)	2.190(3)	Zn(1)- N(1)	2.195(3)
Zn(2)-N(3)	2.198(3)	Zn(1)-N(2)	2.180(3)
O(6)-Zn(2)-O(7)	96.37(9)	O(7)- Zn(2)- N(4)	92.86(13)
O(6)-Zn(2)-O(8)	78.19(12)	O(8)- Zn(2)- N(4)	92.12(13)
O(6)-Zn(2)-O(4)	97.33(8)	O(4)-Zn(2)-N(4)	88.10(11)
O(7)-Zn(2)-O(4)	166.27(9)	O(6)-Zn(2)-N(3)	88.54(11)
O(7)-Zn(2)-O(8)	84.03(9)	O(7)-Zn(2)-N(3)	89.08(13)
O(8)-Zn(2)-O(4)	82.25(9)	O(8)-Zn(2)-N(3)	89.70(13)
O(6)- Zn(2)-N(4)	89.63(11)	O(4)-Zn(2)-N(3)	90.40(11)
N(4)-Zn(2)-N(3)	177.47(11)		
O(3)-Zn(1)-O(9)	100.24(8)	N(2)-Zn(1)-N(1)	172.00(12)
O(3)-Zn(1)-O(1)	169.75(9)	O(3)-Zn(1)-O(2)	113.01(8)
O(9)-Zn(1)-O(1)	90.00(8)	O(9)-Zn(1)-O(2)	146.70(8)
O(3)-Zn(1)-N(2)	93.58(10)	O(1)-Zn(1)-O(2)	56.74(9)
O(9)-Zn(1)-N(2)	92.76(11)	N(2)-Zn(1)-O(2)	83.90(12)
O(1)-Zn(1)-N(2)	85.57(11)	N(1)-Zn(1)-O(2)	89.11(13)
O(3)-Zn(1)-N(1)	92.73(11)	O(1)-Zn(1)-N(1)	87.34(11)
O(9)-Zn(1)-N(1)	90.94(11)		

Table S3 Hydrogen bonding interactions in **1**

D-H···A	D-H (Å)	H···A (Å)	D···A (Å)	<D-H···A (°)
O(8)-H(8A)···O(10)	0.931	1.722	2.620	161.20
O(8)-H(8B)···O(2)	0.930	1.709	2.637	175.41
O(7)-H(7B)···O(9)	0.767	2.089	2.849	170.56
O(7)-H(8)···O(5)	0.819	1.944	2.668	146.93

Table S4 C-H···π interactions in **1**

C-H→ Ring(j)	H···R distance (Å)	C-H···R angle (°)	C···R distance (Å)
C(10)-H(10)→R(1)	2.799	139.30	3.557
C(45)-H(45)→R(3)	3.001	131.14	3.680

R(j) denotes the j-th ring: R(1) = C(25)/C(26)/C(27)/C(28)/C(29)/C(30); R(3) = C(36)/C(37)/C(38)/C(39)/C(40)/C(41)

Table S5 π···π interactions in **1**

Ring(i) → Ring(j)	Distance between the (i,j) ring centroids (Å)
R(1)→R(2)	3.689

R(1) is same as above and R(2) = N(2) /C(20)/C(21)/C(22)/C(23)/C(24).

Table S6 Variation of NICS values (in ppm) with height at different points of the 14 member metal-ligand ring (Maximum negative values of NICS have been given in bold face and values for symmetry unique points are only been given in the table)

	Position (points) over the ring where NICS values are calculated					
Height(Å)	1	2	5	6	10	11
-5.0	-0.305400	-0.285800	-0.258900	-0.281400	-0.266000	-0.295000
-4.5	-0.313000	-0.322100	-0.301700	-0.321800	-0.299000	-0.341800
-4.0	-0.349400	-0.358700	-0.357300	-0.368200	-0.334100	-0.397600
-3.5	-0.383400	-0.389800	-0.432300	-0.420200	-0.369200	-0.463400
-3.0	-0.407900	-0.402700	-0.539100	-0.476600	-0.399600	-0.540100
-2.5	-0.409800	-0.371100	-0.705700	-0.537700	-0.416500	-0.639600
-2.0	-0.382100	-0.245800	-1.015000	-0.626900	-0.405000	-0.818800
-1.5	-0.541000	0.036000	-1.674400	-0.835700	-0.376500	-1.096000
-1.0	-2.286500	0.408800	-2.921700	-1.342300	-0.558000	-1.023900
-0.5	-8.273500	0.570700	-4.262300	-2.838800	-1.292600	0.041300
0.0	-15.22520	0.490000	-3.050800	-7.582500	-1.911000	0.606400
0.5	-11.02260	0.439400	-2.077900	-7.281200	-1.327500	-0.663000
1.0	-3.608000	0.362700	-2.497700	-2.179700	-0.369600	-1.369100
1.5	-0.748900	0.089800	-1.824700	-0.834300	-0.064800	-1.116700
2.0	-0.297400	-0.181700	-1.117000	-0.558400	-0.159800	-0.789000
2.5	-0.319500	-0.321900	-0.735600	-0.486100	-0.262300	-0.614000
3.0	-0.339900	-0.367000	-0.546200	-0.447000	-0.305200	-0.511900
3.5	-0.334200	-0.364100	-0.434300	-0.405200	-0.310100	-0.434500
4.0	-0.314100	-0.340100	-0.358200	-0.361000	-0.296300	-0.371600
4.5	-0.287900	-0.308600	-0.302800	-0.318600	-0.274300	-0.320100
5.0	-0.260100	-0.276200	-0.260200	-0.280300	-0.249700	-0.277700

Table S7 Calculated NICS(0) values at the 14 member metal-ligand ring center and at point(1) for different level of theory

NICS(0) values at the centroid of the 14-member ring			
Method/basis	B3LYP	X3LYP	HF
6-31G(2d)	0.645500	0.648200	1.165800
6-311G	1.153700	1.157500	1.695600
6-31G(d,p)	0.664500	0.667000	1.244800
NICS(0) values at point(1) of the 14-member ring			
6-31G(2d)	-13.904800	-13.938300	-14.664600
6-311G	-15.043000	-15.076800	-15.225200
6-31G(d,p)	-14.244600	-14.275400	-15.080400

Table S8 Component wise variation of NICS values with height at point (1)

Height(Å)	xx	yy	zz	In plane	Out plane	isotropic
0.0	18.5043	29.0102	-1.8388	-15.8382	.6129	-15.2252
0.5	13.0795	19.9753	0.0130	-11.0183	-.0043	-11.0226
1.0	3.4901	4.5689	2.7650	-2.6863	-.9217	-3.6080
1.5	0.2134	-0.8718	2.9050	.2195	-.9683	-0.7489
2.0	-0.2805	-1.6604	2.8331	.6470	-.9444	-0.2974
2.5	-0.3334	-1.5372	2.8289	.6235	-.9429	-0.3195
3.0	-0.3726	-1.3506	2.7431	.5744	-.9144	-0.3399
3.5	-0.3891	-1.1733	2.5652	.5208	-.8551	-0.3342
4.0	-0.3830	-1.0117	2.3371	.4649	-.7790	-0.3141
4.5	-0.3634	-0.8686	2.0956	.4107	-.6985	-0.2879
5.0	-0.3375	-0.7447	1.8625	.3607	-.6208	-0.2601

Table S9 Basis set superposition error (BSSE) corrected binding energies of the C-H $\cdots\pi$ interaction involving 14-member metal-ligand ring and 4-phpy computed at HF/6-31G(d,p) and HF/6-311++G(d,p) level of theory

14-member ring 4-phpy C-H$\cdots\pi$ interaction		
Basis Set	HF/6-31G(d,p)	HF/6-311++G(d,p)
Binding Energy (kcal/mole)	-10.464976	-9.551146
BSSE error (kcal/mole)	1.890166	0.987809
Corrected Binding Energy (kcal/mole)	-8.574810	-8.563337

Table S10 Binding energies of the C-H $\cdots\pi$ interaction involving 14-member metal-ligand ring and 4-phpy, $\pi\cdots\pi$ and two different C-H $\cdots\pi$ interaction among 4-phpy molecules computed at DFT/M06-2X/6-31G(d,p) level of theory

DFT/M06-2X/6-31G(d,p)	
Interaction	Binding energy (kcal/mole)
14member ring CH $\cdots\pi$ interaction	-13.621522
$\pi\cdots\pi$	-7.444478
C-H $\cdots\pi$ (2.79 Å)	-4.607138
C-H $\cdots\pi$ (3 Å)	-3.500504

References

1. M. A. Spackman, and D. Jayatilaka, *CrystEngComm.* 2009, **11**, 19.
2. F. L. Hirshfeld, *Theor. Chim. Acta.* 1977, **44**, 129.
3. H. F. Clausen, M. S. Chevallier, M. A. Spackman, and B. B. Iversen, *New J. Chem.* **2010**, *34*, 193.
4. A. L. Rohl, M. Moret, W. Kaminsky, K. Claborn, J. J. McKinnon, and B. Kahr, *Cryst. Growth Des.* 2008, **8**, 4517.
5. A. Parkin, G. Barr, W. Dong, C. J. Gilmore, D. Jayatilaka, J. J. McKinnon, M. A. Spackman, C. C. Wilson, *CrystEngComm.* 2007, **9**, 648.
6. M. A. Spackman, and J. J. McKinnon, *CrystEngComm.* 2002, **4**, 378.
7. S. K. Wolff, D. J. Grimwood, J. J. McKinnon, D. Jayatilaka, M. A. Spackman, Crystal Explorer 2.0; University of Western Australia: Perth, Australia, **2007**.
<http://hirshfeldsurfacenet.blogspot.com/>